



Dynamic Characterization of InAs/AlGaAs Broadband self-Assembled Quantum Dot Lasers

By D. Ghodsi Nahri, H. Arabshahi

Mashhad Branch, Islamic Azad University, Mashhad, Iran

Abstract - In this research we have solved the rate equations for **InAs/AlGaAs** broadband self-assembled quantum dot (**QD**) laser with considering the homogeneous broadening (**HB**) and inhomogeneous broadening (**IHB**) of the linear optical gain using fourth order Runge-Kutta method. We show that enhancing the injected current results in improving the dynamic characteristics, and increasing the steady-state photons, and show that with increase of the full width at half maximum (**FWHM**) of **HB**, the threshold current, turn-on delay and steady-state photons increase. Our calculation results also show that the simulated broadband self-assembled **QD** laser does not reach the complete steady-state when **HB** is near or equal to **IHB**.

Keywords : *InAs/AlGaAs Broadband Self-assembled quantum dot laser; Dynamic Characterization; Optical gain theory .*

GJSFR-A Classification : *FOR Code : 020604*



DYNAMIC CHARACTERIZATION OF INAS/ALGAAS BROADBAND SELF-ASSEMBLED QUANTUM DOT LASERS

Strictly as per the compliance and regulations of :



Dynamic Characterization of InAs/AlGaAs Broadband self-Assembled Quantum Dot Lasers

D. Ghodsi Nahri^α, H. Arabshahi^α

Abstract - In this research we have solved the rate equations for InAs/AlGaAs broadband self-assembled quantum dot (QD) laser with considering the homogeneous broadening (HB) and inhomogeneous broadening (IHB) of the linear optical gain using fourth order Runge-Kutta method. We show that enhancing the injected current results in improving the dynamic characteristics, and increasing the steady-state photons, and show that with increase of the full width at half maximum (FWHM) of HB, the threshold current, turn-on delay and steady-state photons increase. Our calculation results also show that the simulated broadband self-assembled QD laser does not reach the complete steady-state when HB is near or equal to IHB.

Keywords : InAs/AlGaAs Broadband Self-assembled quantum dot laser; Dynamic Characterization; Optical gain theory;

I. INTRODUCTION

Broadband light-emitting devices, such as super luminescent diodes (SLDs) and external cavity tunable lasers are ideal optical sources for applications in many areas. For example, SLDs can be used in the fields of optical coherence tomography (OCT), fiber-optic gyroscope (FOG) and wavelength-division-multiplexing (WDM) system; while external cavity tunable lasers are used in the fields of optical spectroscopy, biomedical, metrology and dense wavelength division multiplexing (DWDM). It was proposed that the characteristic of size inhomogeneity naturally occurred in self-assembled quantum dots (QDs) grown by Stranski-Krastanow (SK) mode is beneficial to broadening the material gain spectra and therefore, to broadening the lasing emission spectra (Sun et al., 1999). Broadband emitting QD-SLDs and broadband external cavity tunable QD lasers with QD gain medium have been studied (Liu et al., 2005; Lv et al., 2008; Zhang et al., 2004; Zhang et al., 2008). Here, we present simulated results in broadband emitting QD lasers. These InAs/AlGaAs QDs exhibit a broad photoluminescence (PL) full width at half maximum (FWHM) of 80 meV, which is much wider than that grown on GaAs substrate (Lv et al., 2008; Tan et al., 2007; Tan et al., 2008).

The short migration length of indium atoms on AlGaAs surface increases the size dispersion of InAs

QDs, resulting in the broadening of optical gain spectrum. By optimizing the GaAs spacer thickness of multi-stacked InAs/AlGaAs QDs, over 250 μm PL FWHM is achieved. In this paper, considering the homogeneous broadening (HB) and inhomogeneous broadening (IHB) of the optical gain, we have solved the rate equations numerically using fourth order Runge-Kutta method and analyze the dynamics characteristics of InAs/AlGaAs self-assembled QD laser diodes (SAQD-LDs).

II. LINEAR OPTICAL GAIN

Based on the density-matrix theory, the linear optical gain of QD active region is given as

$$g^{(1)}(E) = \frac{2\pi e^2 \hbar N_D}{cn_r e_0 m_0^2} \cdot \frac{|P_{cv}^\sigma|^2 (f_c - f_v)}{E_{cv}} B_{cv}(E - E_{cv}) \quad (1)$$

where n_r is the refractive index, N_D is the volume density of QDs, $|P_{cv}^\sigma|^2$ is the transition matrix element, f_c is the electron occupation function of the conduction-band discrete state, f_v is that of the valence-band discrete state, and E_{cv} is the interband transition energy. The linear optical gain shows the homogeneous broadening of a Lorentz shape as

$$B_{cv}(E - E_{cv}) = \frac{\hbar \gamma_{cv} / \pi}{(E - E_{cv})^2 + (\hbar \gamma_{cv})^2} \quad (2)$$

where FWHM is given as $2\hbar \gamma_{cv}$ with polarization dephasing or scattering rate γ_{cv} . Neglecting the optical-field polarization dependence, the transition matrix element is given as

$$|P_{cv}^\sigma|^2 = |I_{cv}|^2 M^2 \quad (3)$$

where I_{cv} represents the overlap integral between the envelope functions of an electron and a hole, and

$$M^2 = \frac{m_0^2}{12m_e^*} \cdot \frac{E_g (E_g + D)}{E_g + 2D/3} \quad (4)$$

as derived by the first-order k.p is the interaction between the conduction band and valence band. Here,

^{Author ^α} : Department of Physics, Mashhad Branch, Islamic Azad University, Mashhad, Iran.

^{Author ^β} : Department of Physics, Payame Noor University, PO Box 19395-3697, Tehran, Iran . E-mail : arabshahi@um.ac.ir

E_g is the band gap, m_e^* is the electron effective mass, D is the spin-orbit interaction energy of the QD material. Equation 3 holds as long as we consider QDs with a nearly symmetrical shape (Sugawara, 1999; Sugawara et al., 2000). In actual SAQD-LDs, we should rewrite the linear optical gain formula of equation 1 by taking into account inhomogeneous broadening due to the QD size and composition fluctuation in terms of a convolution integral as

$$g^{(1)}(E) = \frac{2\pi e^2 \hbar N_D}{cn_r \epsilon_0 m_0^2} \int_{-\infty}^{\infty} \frac{|p_{cv}^\sigma|^2}{E_{cv}} (f_c(E') - f_v(E')) \times B_{cv}(E - E') G(E' - E_{cv}) dE' \quad (5)$$

where E_{cv} is the center of the energy distribution function of each interband transition, $f_c(E')$ is the electron occupation function of the conduction-band discrete state of the QDs with the interband transition energy of E' , and $f_v(E')$ is that of the valence band discrete state. The energy fluctuation of QDs are represented by $G(E' - E_{cv})$ that takes a Gaussian distribution function as

$$G(E' - E_{cv}) = \frac{1}{\sqrt{2\pi}\xi_0} \exp(-(E' - E_{cv})^2 / 2\xi_0^2) \quad (6)$$

Whose FWHM is given by $G_0 = 2.35\xi_0$. The width G_0 usually depends on the band index c and (Sugawara, 1999; Sugawara et al., 2000).

III. RATE EQUATIONS

The most popular and useful way to deal with carrier and photon dynamics in lasers is to solve rate equations for carrier and photons (Markus et al., 2003; Sugawara, 1999; Sugawara et al., 2000; Tan et al., 2007; Tan et al., 2008). In our model, we consider an electron and a hole as an exciton, thus, the relaxation means the process that both an electron and a hole relax into the ground state simultaneously to form an exciton. We assume that the charge neutrality always holds in each QD.

In order to describe the interaction between the QDs with different resonant energies through photons, we divide the QD ensemble into $j=1, 2, \dots, 2M+1$ groups, depending on their resonant energies for the interband transition over the longitudinal cavity photon modes.

$j = M$ corresponds to the group and the mode with the central transition energy E_{cv} . We take the energy width of each group equal to the mode separation of the longitudinal cavity photon modes which equals to

$$D_E = ch / 2n_r L_{ca} \quad (7)$$

where L_{ca} is the cavity length. The energy of the j^{th} QD group is represented by

$$E_j = E_{cv} - (M - j)D_E \quad (8)$$

where $j = 1, 2, \dots, 2M + 1$. The QD density j^{th} QD group is given as

$$N_D G_j = N_D G(E_j - E_{cv}) D_E \quad (9)$$

Let N_j be the carrier number in j^{th} QD group, According to Pauli's exclusion principle, the occupation probability in the ground state of the j^{th} QD group is defined as

$$P_j = N_j / 2N_D V_a G_j \quad (10)$$

where V_a is the active region volume. The rate equations are as follows (Grundmann, 2002; Sugawara, 1995; Sugawara et al., 1997; Sugawara et al., 2000; Sugawara et al., 2005; Tan et al., 2008)

$$\frac{dN_s}{dt} = \frac{I}{e} - \frac{N_s}{\tau_s} - \frac{N_s}{\tau_{sr}} + \frac{N_w}{\tau_{we}}$$

$$\frac{dN_w}{dt} = \frac{NN_s}{\tau_s} + \sum_j \frac{N_j}{\tau_e D_g} - \frac{N_w}{\tau_{wr}} - \frac{N_w}{\tau_{we}} - \frac{N_w}{\bar{\tau}_d}$$

$$\frac{dN_j}{dt} = \frac{N_w G_j}{\tau_{dj}} - \frac{N_j}{\tau_r} - \frac{N_j}{\tau_e D_g} - \frac{c\Gamma}{n_r} g^{(1)}(E) S_m$$

$$\frac{dS_m}{dt} = \frac{\beta N_j}{\tau_r} + \frac{c\Gamma}{n_r} g^{(1)}(E) S_m - S_m / \tau_p \quad (11)$$

where N_s , N_w , and N_j are the carrier numbers in separate confinement heterostructure (SCH) layer, wetting layer (WL) and j^{th} QD group, respectively, S_m is the photon number of m^{th} mode, where $m=1, 2, \dots, 2M+1$, I is the injected current, G_j is the fraction of the j^{th} QD group type within an ensemble of different dot size population, e is the electron charge, D_g is the degeneracy of the QD ground state without spin, b is the spontaneous-emission coupling efficiency to the lasing mode. $g_{mj}^{(1)}$ is the linear optical gain which the j^{th} QD group gives to the m^{th} mode photons where is represented by

$$g_{mj}^{(1)}(E) = \frac{2\pi e^2 \hbar N_D}{cn_r \epsilon_0 m_0^2} \cdot \frac{|p_{cv}^\sigma|^2}{E_{cv}} (2p_j - 1). \quad (12)$$

the related time constants are as τ_s , diffusion in the SCH region, τ_{sr} , carrier recombination in the SCH region, τ_{we} , carrier reexcitation from the WL to the SCH region, τ_{wr} , carrier recombination in the WL, τ_{dj} , carrier relaxation into the j^{th} QD group, τ_r , carrier recombination in the QDs, τ_p , photon lifetime in the cavity, The average carrier relaxation lifetime, $\bar{\tau}_d$, is given as

$$\tau_d^{-1} = \sum_j \tau_{dj}^{-1} G_j = \tau_{d0}^{-1} (1 - P_j) G_j \quad (13)$$

where τ_{do} is the initial carrier relaxation lifetime. The photon lifetime in the cavity is

$$\tau_p^{-1} = (c/n_r)[\alpha_i + \ln(1/R_1R_2)/2L_{ca}] \quad (14)$$

where R_1 and R_2 are the cavity mirror reflectivities, and α_i is the internal loss. The laser output power of the m^{th} mode from one cavity mirror is given a

$$I_m = \hbar\omega_m c S_m \ln(1/R) / (2L_{ca} n_r) \quad (15)$$

where ω_m is the emitted photon frequency, and R is R_1 or R_2 . We solved the rate equations numerically using fourth order Runge-Kutta method to

obtain the carrier and photon characteristics by supplying the step-like current at the time of $t = 0$. The system reaches the steady-state after finishing the relaxation oscillation.

IV. SIMULATION RESULTS AND DISCUSSION

We have solved the rate equations 11 using numeric method of Runge-Kutta and simulated the carrier and photon characteristics. Figure 1 shows the simulated results of carrier characteristics at the FWHM of IHB 80 meV for different injected currents $I=1.5, 2, 2.5, 5,$ and 10 mA and at the FWHM of HB $2\hbar\gamma_{cv} = 80$ meV.

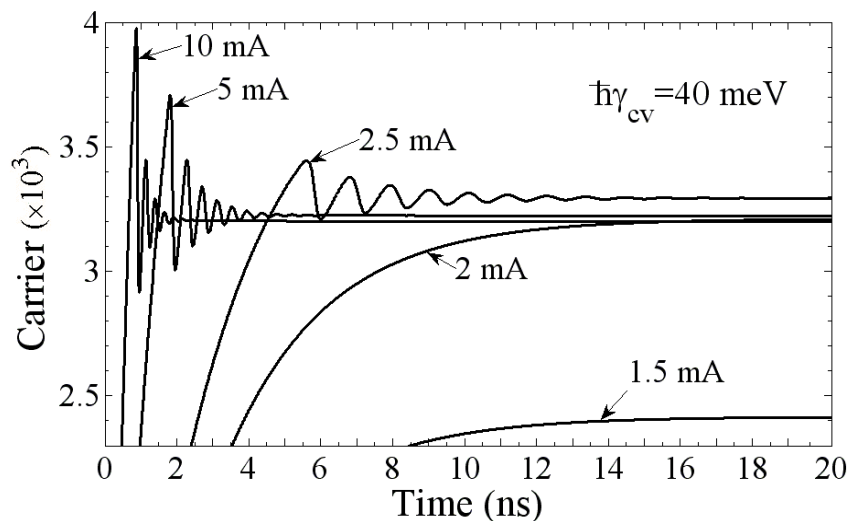


Fig. 1 : Simulated results of carrier characteristics at the FWHM of IHB 80 meV for different injected currents of 1.5, 2, 2.5, 5, and 10 mA and at the FWHM of HB 20 meV.

As shown in figure 1, with increasing the injected current, maximum of the relaxation oscillation magnitude and relaxation oscillation frequency increase.

Figure 2 shows the simulated results of photon characteristics at the FWHM of IHB 80 meV for different injected currents $I=2, 2.5, 5$ and 10 mA and at the FWHM of HB 24, 40, 56, and 80 meV.

As shown in figure 2, the steady-state photons increase as the injected current is increased. This is because, as the injected current increases, the QD carriers increase that it results in increasing the cavity lasing photons, these increased photons that we call "early photons" lead to enhancing the stimulated emission rate, as a result, the QD carriers decrease (Figure 1) and the lasing photons increase at the new steady-state. With increasing the injected current, turn on delay decreases, this occurs because the required carriers for beginning of the relaxation oscillation are supplied earlier. Relaxation oscillation frequency and maximum of the relaxation oscillation magnitude also enhance as the current elevates. Further increase of early photons leads to further enhancement of the

relaxation oscillation frequency and maximum of the relaxation oscillation magnitude. Because, further increase of the stimulated emission rate leads to the quicker light amplification and decreasing the cavity photon lifetime as a result the relaxation oscillation frequency increases and the laser reaches the steady-state earlier. As the FWHM of HB increases from a to d, turn on delay and the threshold current increase, because density of states (DOS) of the central group increase as a result the required carrier number for beginning of lasing emission increases and are supplied later. Steady-state photons except to figure 2a at the current $I=2.5$ mA increase due to increasing the QDs lying within the HB of the central mode.

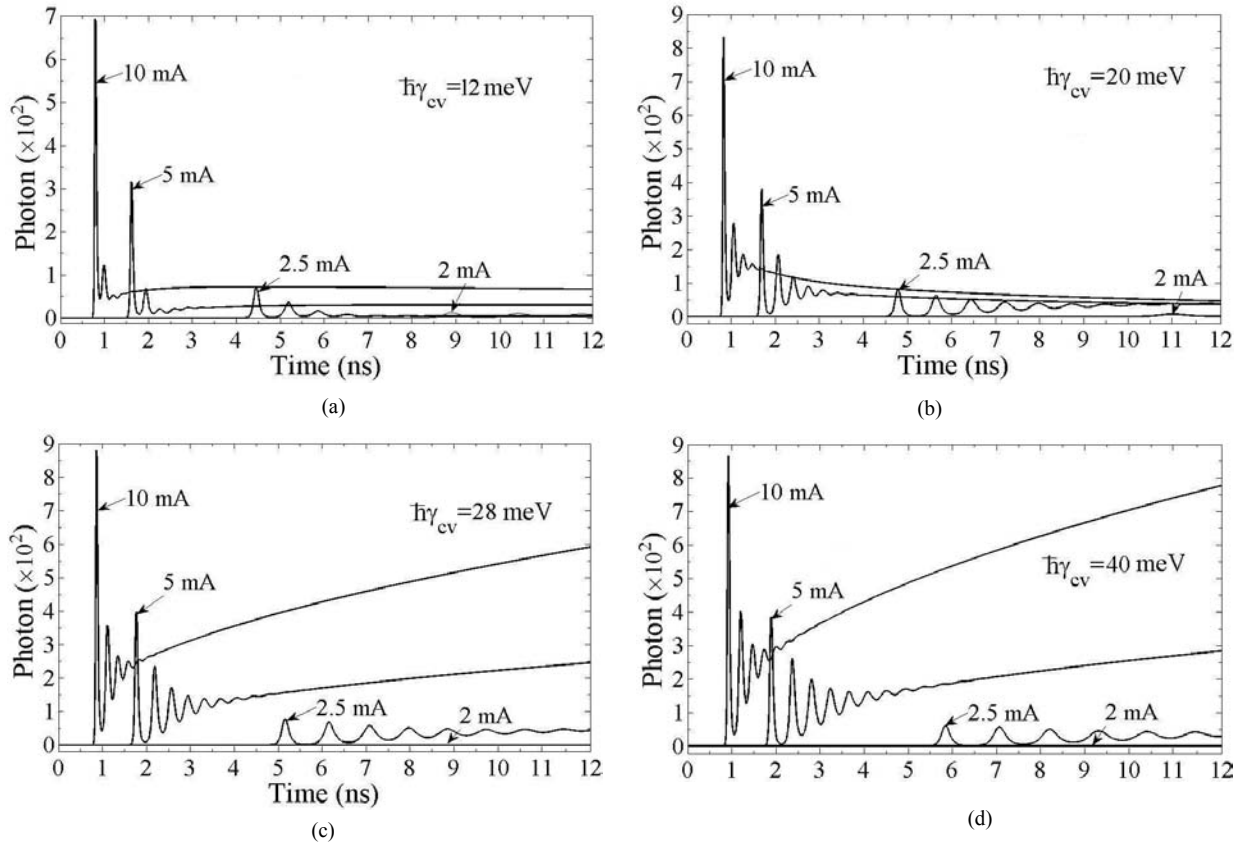


Fig. 2 : Simulated results of photon characteristics at the FWHM of IHB 80 meV for different injected currents $I=2, 2.5, 5,$ and 10 mA when the FWHM of HB is $24, 40, 56$ and 80 meV.

Enhancing of the HB up to a special value for a specific current (for example, in figure 2a, up to $\hbar\gamma_{cv} = 12$ meV for $I=2$ mA) leads to increasing of maximum of the relaxation oscillation magnitude and the steady-state photons, because the central group DOS and thus the central group carriers enhance. Further elevating of the HB results in heightening of the empty DOS at the central group (decreasing of the population

inversion) and decreasing of maximum of the relaxation oscillation magnitude and the steady-state photons (see Figure 3). As shown in Figure 3, at the injected current $I=2$ mA, with increasing of the FWHM of HB from 24 meV, the steady-state photons decreases as the population inversion is provided at a higher current at HB more than 56 meV and as a result, the threshold current elevates.

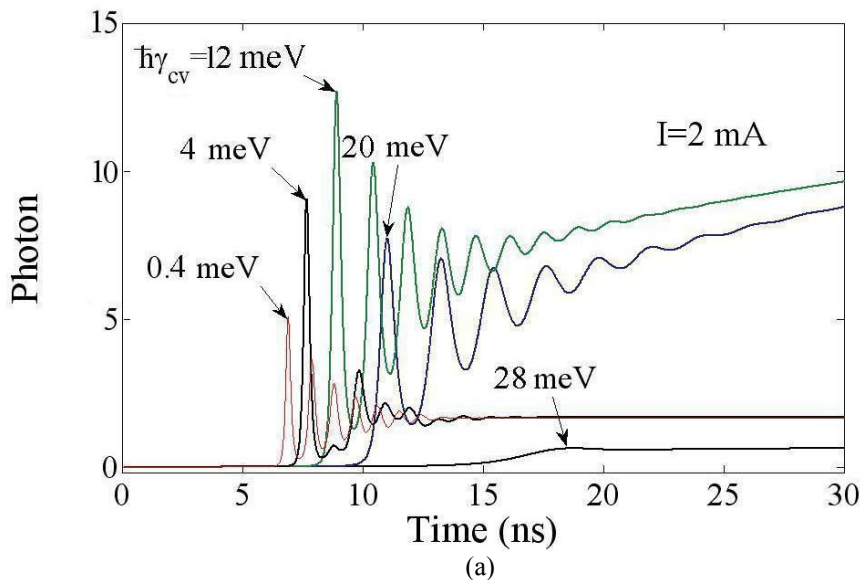


Fig. 3 : Photon-characteristics at the FWHM of IHB 80 meV for $I=2$ mA and at $\hbar\gamma_{cv}= 0.4, 4, 12, 20,$ and 28 meV.

Figure 4 shows other illustration from photon-characteristics at the FWHM of IHB 80 meV for different injected currents $I=2, 2.5, 5,$ and 10 mA at a longer calculating time and at (a) $\hbar\gamma_{cv}=12\text{ meV}$, (b) 20 meV , (c) 28 meV , and (d) 40 meV .

As shown in figure 4a, the steady-state photons at $I=2.5\text{ mA}$ are lesser than that of $I=2\text{ mA}$. Lasing photons at $I=5$ and 10 mA reach the complete steady state after 100 ns and 60 ns, respectively. As it is shown in figure 4b, the lasing photons at $I=5$ and 10 mA decrease as the time increases and they become lesser than that of $I=2\text{ mA}$ after 45 ns, they do not reach the

complete steady-state even after 100 ns. Lasing photons at 10 mA become lesser than that of 5 mA after 30 ns. Lasing photons at $I=2.5\text{ mA}$ increase as the time enhances, and they do not reach the complete steady-state after 100 ns. As it is shown in figure 4c, the lasing photons at $I=2.5\text{ mA}$ reach the complete steady-state after 80 ns, but, the lasing photons at $I=5$ and 10 mA do not reach the complete steady-state and they elevate as the time increases. As it is shown in figure 4d, the lasing photons at $I=5$ and 10 mA do not reach the steady-state after 300 ns. These non steady-states are due to not considering the gain saturation effect.

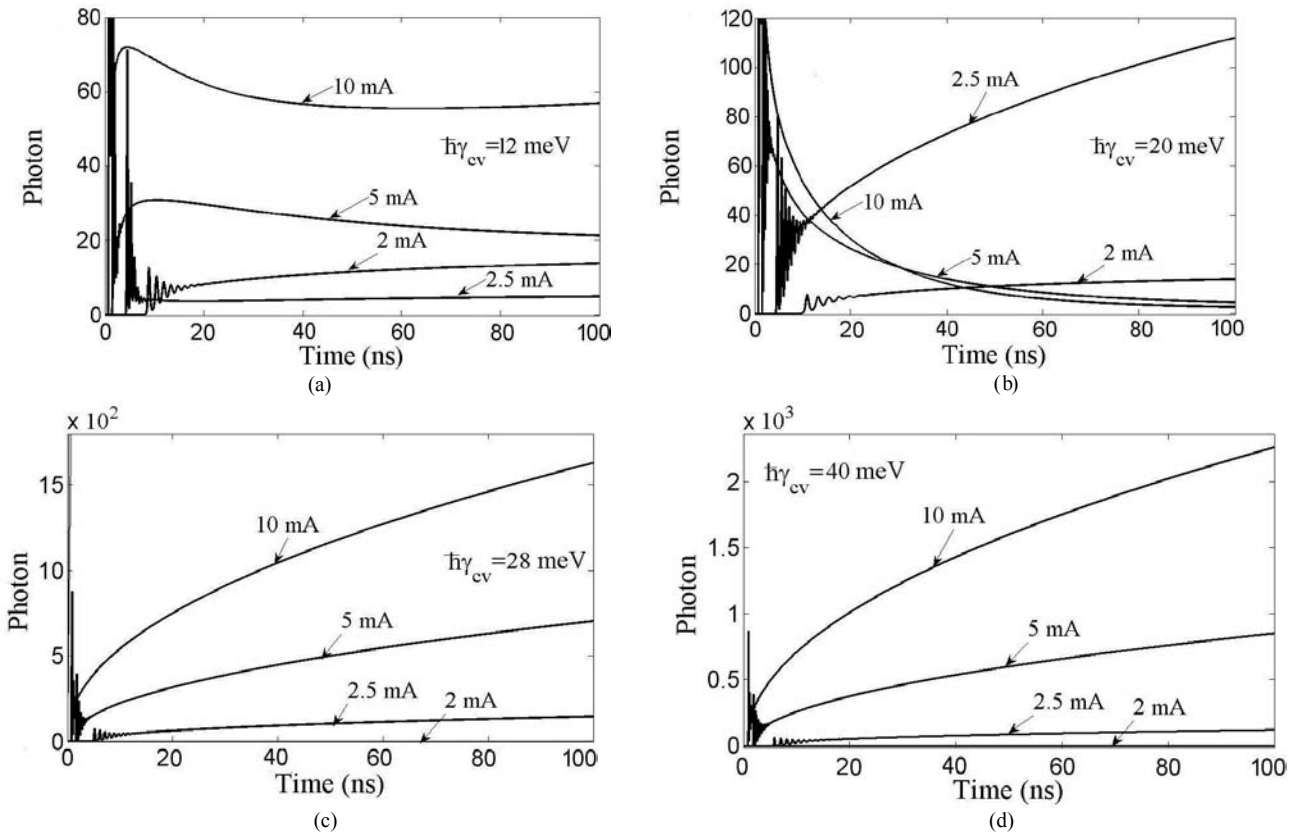


Fig. 4 : Other illustration from photon-characteristics for different injected currents $I=2, 2.5, 5,$ and 10 mA at 100 ns and at (a) $\hbar\gamma_{cv} = 12\text{ meV}$ (b) 20 meV , (c) 28 meV and (d) 40 meV .

V. CONCLUSION

InAs/AlGaAs self-assembled QD lasers with broadband emitting spectra have been studied. Considering the HB and IHB of the linear optical gain, we have solved the rate equations numerically using fourth order Runge-Kutta method and analyzed the dynamic characteristics of InAs/AlGaAs broadband SAQD-LDs. Dynamic characteristics and steady-state photons improve as the current increases. Turn-on delay, the threshold current and steady-state photons increase as the HB enhances. In addition, the SAQD-LD does not reach the complete steady-state when HB is near or equal to IHB.

REFERENCES RÉFÉRENCES REFERENCIAS

1. Grundmann M (2002). Nano Optoelectronics. Springer, New York.
2. Liu N, Jin P and Wang Z (2005). InAs/GaAs quantum-dot super luminescent diodes with 110 nm bandwidth. *Electron. Lett.*, 41: 1400-1402.
3. Lv, X Q, Liu N, Jin P and Wang Z (2008). Broadband emitting super luminescent diodes with InAs quantum dots in AlGaAs matrix. *IEEE Photon. Technol. Lett.*, 20: 1742-1744.
4. Markus A, Chen J, Gauthier-Lafaye O and Fiore A (2003). Impact of intraband relaxation on the performance of a quantum-dot laser. *IEEE J. Sel. Top Quantum electron.*, 9: 1308-1314.

5. Sugawara M (1995). Theory of spontaneous-emission lifetime of Wannier in mesoscopic semiconductor quantum disks. *Phys. Rev. B Condens. Matter.*, 51: 10743-10754.
6. Sugawara M, Mukai K and Shoji H (1997). Effect of phonon bottleneck on quantum-dot laser performance. *Applied Phys. Lett.*, 71: 2791-2793.
7. Sugawara M (1999). *Self -Assembled InGaAs/GaAs Quantum Dots*. Academic Press 60.
8. Sugawara M, Mukai K and Ishikawa H (2000). Effect of homogeneous broadening of optical gain on lasing spectra in self-assembled $\text{In}_x\text{Ga}_{1-x}\text{As}/\text{GaAs}$ quantum dot lasers. *Phys. Rev. B*, 61: 7595-7603.
9. Sugawara M and Ishida M (2005). Modeling room-temperature lasing spectra of 1.3- μm self-assembled InAs/GaAs quantum-dot lasers: Homogeneous broadening of optical gain under current injection. *Applied Phys.*, 97: 043523-043530.
10. Sun Z, Ding D, Gong Q, Zhou W and Wang Z (1999). Quantum-dot superluminescent diode: A proposal for an ultra-wide output spectrum. *Opt. Quantum Electron.*, 31: 1235-1246.
11. Tan C, Wang Y and Ooi B (2007). Role of optical gain broadening in the broadband semiconductor quantum-dot laser. *Applied Phys. Lett.*, 91: 061117-061119.
12. Tan C, Wang Y and Ooi B (2008). The role of optical gain broadening in the ultrabroadband $\text{InGaAs}/\text{GaAs}$ interband quantum-dot laser. *Comput. Matter. Sci.*, 44: 167-173.
13. Zhang Z, Wang Z and Liu F (2004). High performance Quantum - dot superluminescent diodes. *IEEE Photon. Technol. Lett.*, 16: 27-29.
14. Zang Z and Wang Z Q (2008). High-power quantum-dot superluminescent LED with broadband drive current insensitive emission spectra using tapered active region. *IEEE Photon. Technol. Lett.*, 20: 782-784.

